Solid-state co-extrusion of nylon-6 gel

Hoe Hin Chuah and Roger S. Porter
Materials Research Laboratory, Polymer Science and Engineering Department, University of Massachusetts, Amherst, Massachusetts 01003, USA
(Received 28 December 1984; revised 3 September 1985)

A partially dried nylon-6 gel has been drawn at 150°C and to draw ratio 5.7×, by a split billet co-extrusion technique in an Instron capillary rheometer. The gel was prepared by dissolving nylon-6 in benzyl alcohol at 165°C and cooling to gel at room temperature. On removing solvent, preorientation was introduced into the gel with the *b*-chain axis weakly oriented perpendicular to the gel surface. Drawing produces double orientation. One population of the crystals is oriented with chain axes in the draw direction, as in the usual uniaxial drawing. The second population has its chain axes oriented perpendicular to draw direction. From birefringence, wide- and small-angle X-ray scattering studies, a deformation mechanism for the double orientation was proposed. Thermal and mechanical properties were also studied. Annealing at 190°C produced partial reorientation of the second crystals resulting in a more complex orientation.

(Keywords: solid-state co-extrusion; nylon-6 gel; deformation mechanism; double orientation; annealing)

INTRODUCTION

Pennings and coworkers[1] reported ultra-high modulus polyethylene fibre of >100 GPa made by a continuous growth technique, in either a Poiseuille or Couette flow. It was recognized that the fibre was produced from a gel layer where the fibrous seed-crystal was attached. The success of this technique is due to reduced molecular entanglements in the gel and to the efficient stretching of chains in a flow field. Subsequently, the potential of a gel state as a route to high modulus fibre has received considerable attention[2,3]. Smith and Lemstra[4] further extended the technique to ultra-draw a dried, moulded or cast polyethylene gel film. Such dried gel was reported to draw well, even up to 20× at room temperature[5]. Other polymers that form gels, polypropylene[6,7] and poly(vinyl alcohol)[8], have also been reported to draw well by this method, resulting in high modulus fibres.

Lloyd[9] noted nearly 60 years ago that the term gel is easier to recognize than to define. This, to some extent, is still true today. In the present context, gel refers to a macroscopically coherent structure connected by spatial junction points, trapping a large amount of solvent.

In general, gels are not formed from a good solvent. Gelation occurs when solubility changes by either varying temperature or adding a poor solvent to a polymer solution[10]. Apart from gelation involving flow, polymer can also gel under quiescent conditions as when a hot, semi-dilute solution is rapidly cooled. Gelation of semi-crystalline polymer has long been recognized as a crystallization process[11]. One molecular chain may form cohesive junction points with others at several loci along the chain to form a molecular network. If the junction is very small, the gel approaches a homogeneous one-phase system. With several chain segments arranging in lateral order, the junction can then form micellar crystals. It was suggested by Keller[12] that micellar crystals are responsible for gel formation for polymers such as polyethylene, poly(vinyl chloride) and isotactic polystyrene. Micellar crystals can also be mixed with lamellar crystals, and possibly some with tie molecules, giving gel connectedness. Microscopy study of polyethylene gel by Lemstra and Smith[13] however revealed lamellar crystals acting as the spatial junctions for gelation as opposed to the shish-kebab structure obtained in a flowing solution[2].

Nylon-6 forms a gel when its solution in hot benzyl alcohol is cooled to room temperature. Stamhuis and Pennings[14] investigated the morphology by electron microscopy and found an interlacement of several μm long thin fibrillar crystals of 100~200 Å lateral dimension, aggregated into ribbons of high aspect ratio. These fibrillar crystals have their chain axis perpendicular to the surface and the hydrogen bond direction in the long axes of the crystal. The interlacement forms physical entanglements, traps solvent and forms a gel even at concentration as low as 0.1 wt%, well below the coil overlap conditions. Gelation in this case is different from the micellar crystal or crystallite type of gel but analogous to the gelation of rodlike particles, which forms a continuous framework through physical contacts[11]. Thus the fibrillar crystals of the nylon-6 gel do not necessarily have reduced molecular entanglements as in polyethylene gel.

The nylon-6 gel was reported to be brittle and could not be drawn[14]. However, the co-extrusion method developed in this laboratory has successfully drawn several brittle polymers[15]. By our drawing methods, there is a simultaneous compression and extension in a conical die with the deformed polymer film supported on each face by a surface of poly(oxymethylene) coextrudate. We are consequently able to draw a partially dried nylon-6 gel up to 5.7×. This paper investigates the drawing behaviour and properties of the drawn gel. A deformation mechanism is proposed for the observed double orientation.

0032-3861/86/071022-08$03.00

EXPERIMENTAL

Pellets of high molecular weight nylon-6 ($[\eta] = 4.67$ dl g^{-1} in 85% formic acid, $M_v = 183\,000$, Allied Chemicals) were dissolved in benzyl alcohol at 5 wt% concentration at 165°C. The solution was stirred for 1 h under a N_2 atmosphere. It was then poured into a petri dish lined with filter paper, where it gelled at room temperature. Solvent was subsequently removed by blotting with layers of filter paper applied at ever increasing pressure, up to 40 MPa in a press. This was repeated until a partially dried gel was obtained. Further solvent was removed under vacuum at 40°C to give final gel with ~20 wt% solvent, acting as plasticizer and giving ductility to the film. A thoroughly dried film is brittle.

A 2 mm wide strip of the gel film, dried as above, was placed in the centre of a split poly(oxymethylene) billet and co-extruded through a conical die of 20° entrance angle in an Instron capillary rheometer at 150°C[16]. This extrusion temperature was chosen as a convenience as poly(oxymethylene) melts at ~160°C and draws easily up to 8×. Draw ratio was measured from the displacement of lateral markers placed on the gel prior to draw. About 10% solvent remained in the extrudate and was removed in vacuum oven at 100°C for 48 h.

Thermal behaviour was characterized with a Perkin–Elmer Differential Scanning Calorimeter-II (DSC) with heating rate of 10°C min^{-1}. Indium and tin were used for calibration. Tensile modulus at 0.1% strain was measured using a floor model Instron tensile tester at a strain rate of 0.01 min^{-1}.

Total orientation of the drawn gel was measured by birefringence using an Ehringhaus calcspar compensator in a Zeiss optical microscope. As the drawn gel developed double orientation, a Zeiss universal stage was used to measure birefringence as a function of tilt angle, ϕ, by rotation about the draw axis[17,18]. The sample was placed in between glass hemisphere of 1.555 refractive index for beam convergence. This limits ϕ measured up to 40°.

Birefringence, Δ_i, at the tilt angle ϕ is given as

$$\Delta_i = \frac{R_\phi}{t}\left(1 - \frac{\sin^2\phi}{n^2}\right)^{1/2}$$

where R_ϕ is the retardation, t is film thickness and n the refractive index of the film.

A flat film Statton camera with sample-to-film distances of 5 cm and 32 cm was used to obtain wide- and small-angle X-ray diffraction (WAXD and SAXS) photographs respectively using CuKα radiation with Ni filter, operating at 40 kV and 30 mA. Density of X-ray film was measured with a Nonius microdensitometer.

Crystallite size in a-axis direction was measured from broadening of (200) diffraction with a Siemens D-500 diffractometer equipped with a scintillation counter. The divergence and anti-scatter slits were 0.3° and the receiving slit was 0.015°. Scanning rate was 0.2° 2θ min^{-1}. The hexamethylene tetramine peak at 17.8° 2θ was used to correct for instrumental broadening. Scherrer's equation was used to calculate the crystallite size.

RESULTS AND DISCUSSION

Characterization of undrawn gel film

Nylon-6 was found to gel into the α-crystals with high crystallinity, 55%, as measured from d.s.c. This crystal form is the one normally obtained by solution crystallization. A d.s.c. scan of a thoroughly dried gel (*Figure 1*) shows two prominent endotherms with peak melting points at 210°C and 219.5°C. The two endotherms have approximately equal peak area. Double endotherms in solution crystallized nylon-6 have previously been reported[19,20]. Kyotani[20] attributed the low temperature endotherm to lamellar crystals which crystallized during cooling the solution to room temperature after isothermal crystallization. Prolonging the isothermal crystallization time was reported to give only a single high temperature endotherm of more perfect, larger lamellar crystals. However, Stamhuis and Pennings[14] had shown that nylon-6 gel morphology exhibits long ribbons of aggregated fibrillar crystals. This fibrillar morphology was also obtained from stirred crystallization in 1,2,6-hexanetriol solution giving a melting point of 223°C ~ 224°C[20]. Thus in the present gel system, the observed high temperature endotherm is likely for fibrillar crystals mixed with possibly some large lamellar crystals.

Figure 2 shows WAXD and SAXS photographs of a dried gel film prior to extrusion draw. The X-ray beam was directed perpendicular and parallel to the film plane. Viewed perpendicularly, *Figure 2(a)*, there are two (200) and (002) isotropic rings. The inner (200) reflection is much more intense than the outer (002) reflection. SAXS however shows that over a larger range, the system is not entirely isotropic as indicated by an uneven intensity for the ring. When the X-ray beam is placed parallel to the

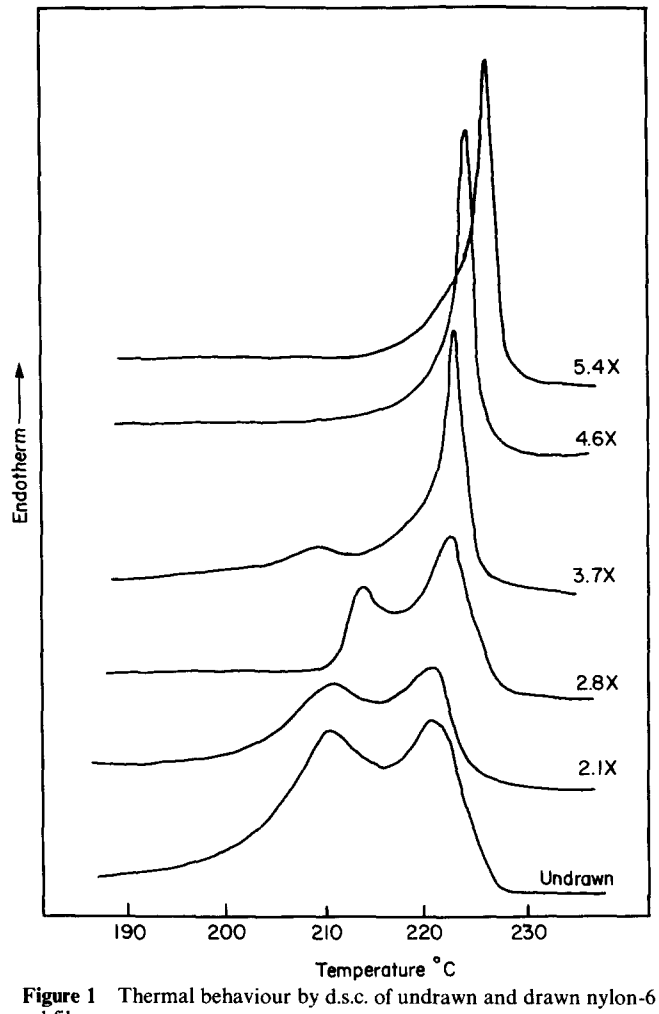

Figure 1 Thermal behaviour by d.s.c. of undrawn and drawn nylon-6 gel film

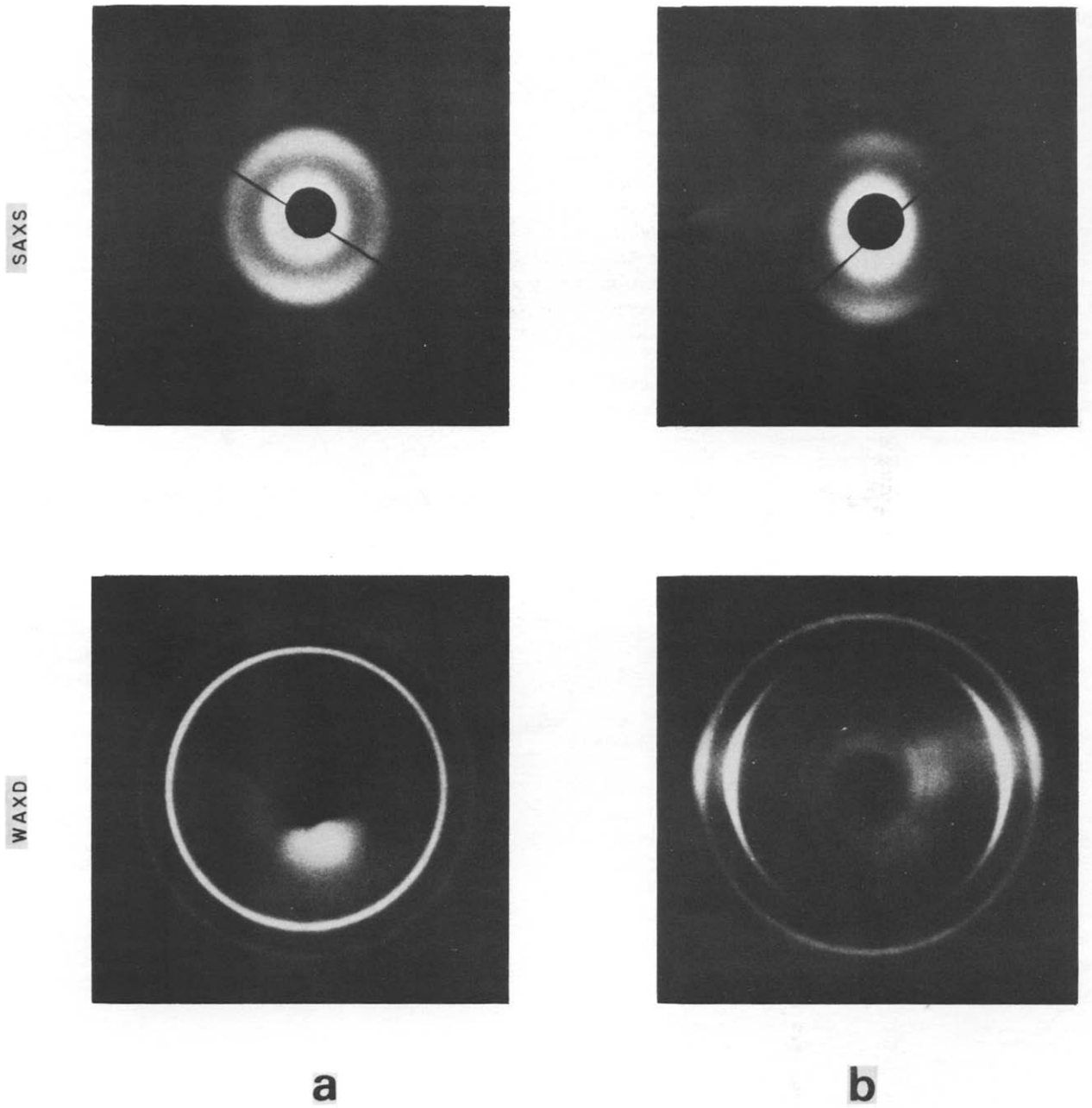

Figure 2 WAXD and SAXS photographs of undrawn, dried gel with beam (a) normal and (b) parallel to film plane

film plane, *Figure 2(b)*, wide equatorial (200) and (002) arcs are superimposed on the Debye rings, and SAXS shows wide meridional maxima. These indicate that orientation has been introduced in the gel film with the *b*-chain axis weakly oriented perpendicular to the film plane as a result of squeezing during solvent removal. This is confirmed by a WAXD photograph, taken with the beam parallel to an unpressed gel, which shows only isotropic rings. The preorientation, however, does not cause double orientation of crystals in the drawn gel, to be discussed later. It does affect the distribution of crystals when viewed parallel to the draw direction.

Properties of drawn gel film

Thermal evaluation by d.s.c. of the drawn gel film is shown in *Figure 1*. With increasing draw ratio, the low temperature endotherm decreases in magnitude and shifts slightly towards higher temperature, completely disappearing at a draw 4.6× and higher, leaving only a single endotherm with a peak melting at 224°C at draw 5.4×. The disappearance of the low temperature endotherm must be due to the destruction of the lamellar crystals on draw leading to their incorporation in a newly-formed fibrous morphology. The fate of the ribbons of fibrillar crystals on draw is not revealed by d.s.c. since their melting point is in the same range as that of the drawn fibrous morphology[21]. The fraction of crystallinity decreases with draw by ~9% at the highest draw ratio 5.7× (*Table 1*) with yet no satisfactory explanation. An initial decrease has been reported by Urbanczyk[22] and attributed to crystal transition on deformation. Major crystallinity decrease has also been reported for poly(ethylene terephthalate)[23] and polyethylene[24]. The decrease in polyethylene was due to the dilation of the *a*-axes, resulting in a decrease in crystal density on drawing[25].

Table 1 Change of crystallinity as a function of draw ratio as measured by d.s.c.

Draw ratio	% Crystallinity
Undrawn	55.0
2.1	47.8
2.9	48.7
3.7	47.3
4.6	45.6
5.4	45.0
5.7	45.5

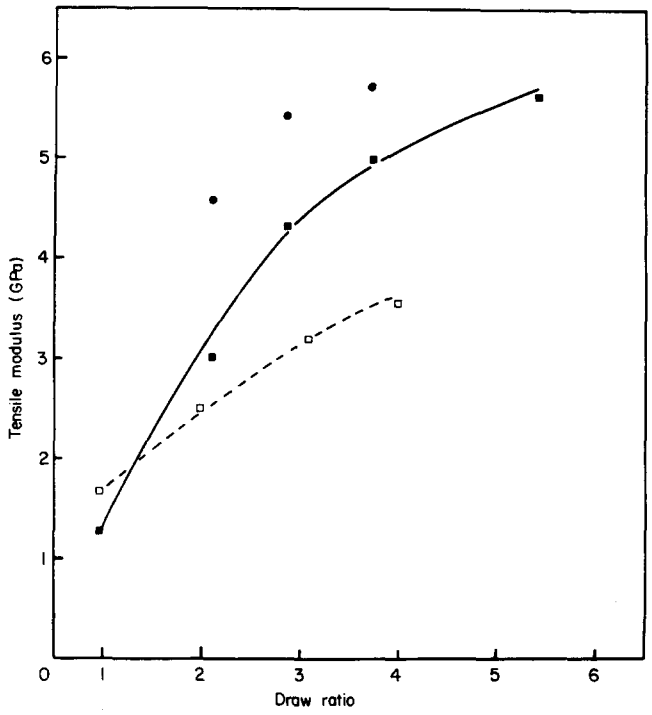

Figure 3 Tensile modulus of nylon-6 as a function of draw ratio: (□) solvent-cast film; (■) gel film; (●) gel film after annealing

As pointed out earlier, nylon-6 gel formation does not necessarily result in significant reduced molecular entanglement. The maximum draw ratio of 5.7× obtained here is comparable to those previously reported for nylon-6. Tensile moduli of the drawn gel are shown in *Figure 3*. The moduli of a solvent cast film, drawn under similar conditions, shown by the broken line, are included for comparison. At equivalent draw ratios, the modulus of gel film is modestly higher, reaching 5.6 GPa. Annealing at 190°C under tension shows a slight improvement in the modulus, from 5.0 GPa to 5.7 GPa for draw ratio 3.7×.

The total orientation of both the amorphous and crystalline chains was measured by birefringence (*Figure 4*). The undrawn film shows birefringence of 0.011, which is due to orientation introduced during solvent removal. On drawing, the birefringence increases almost linearly to 0.044 at a draw of 5.7×. By comparison, birefringence of the drawn cast film increases sharply at low draw, reaching a plateau of 0.061 at a draw of 3.5× with values consistent with reports on uniaxially drawn nylon-6 film and filament[26]. The lower birefringence of the drawn gel can be explained. Investigations by both WAXD and SAXS show double orientation; there are two populations of crystals with chain axis either parallel or perpendicular to the draw direction. Since birefringence is the difference in refractive indices along and perpendicular to draw, the presence of a crystal fraction with chain axis perpendicular to draw direction reduces the birefringence.

Deformation mechanism

Double orientation on deformation has been reported for several types of gel[27-29]. An explanation offered by Keller[12] is that the initial gel contains a mixture of both micellar and lamellar crystals. On deformation, the micellar crystals orient with their chain axis in the draw direction as in the stretching of a network. Conversely, the lamellar crystals align with their lamellar planes along the stretch direction and therefore with chain axis perpendicular to draw. An unconnected lamellar crystal could possibly orient this way on drawing without much chain unravelling. It is less likely that lamellar crystals with molecular weight $\sim 10^6$, and possibly interconnected, will do so rather than orienting with chain unravelling to form fibrous morphology in the draw direction.

Since nylon-6 gel has an interlacement of fibrillar crystals, a different morphology from a polyethylene gel, an alternative mechanism is proposed. Orientation of crystals with chain axes in the draw direction arises from the fibrous morphology normally observed in uniaxial drawing. The second orientation of crystals, with chain axis perpendicular to draw direction, is from the fibrillar crystals which have chain axis perpendicular to the surface plane and hydrogen bonding in the long axis. They rotate when subjected to torque on deformation so that the long axis (*a*-axis) is preferentially oriented in the draw direction. This is similar to the rotation of needle shaped crystals in segmented polyurethane to give a negative orientation as proposed by Bonart[30]. This proposed mechanism is shown to be consistent with the birefringence, WAXD and SAXS results as a function of draw ratio.

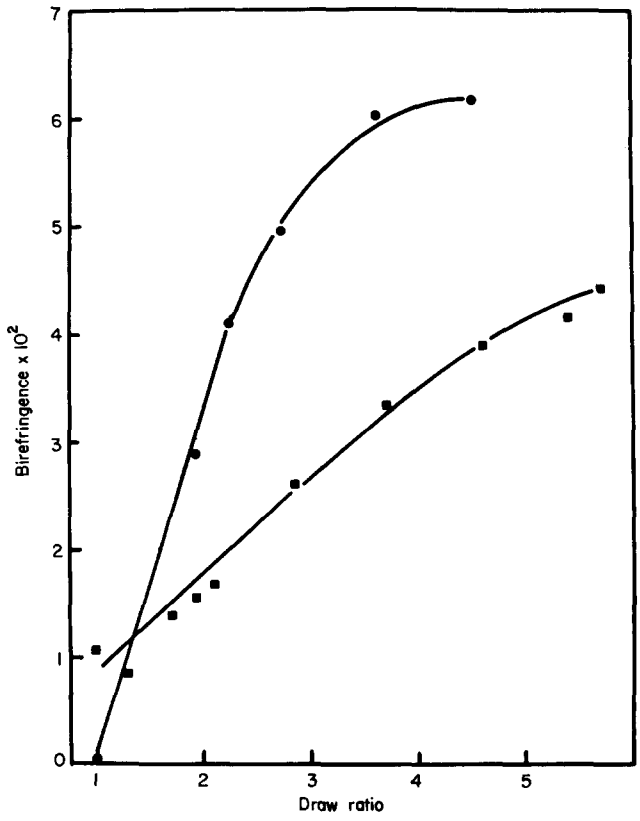

Figure 4 Birefringence of nylon-6 as a function of draw ratio: (■) gel film; (●) solvent-cast film

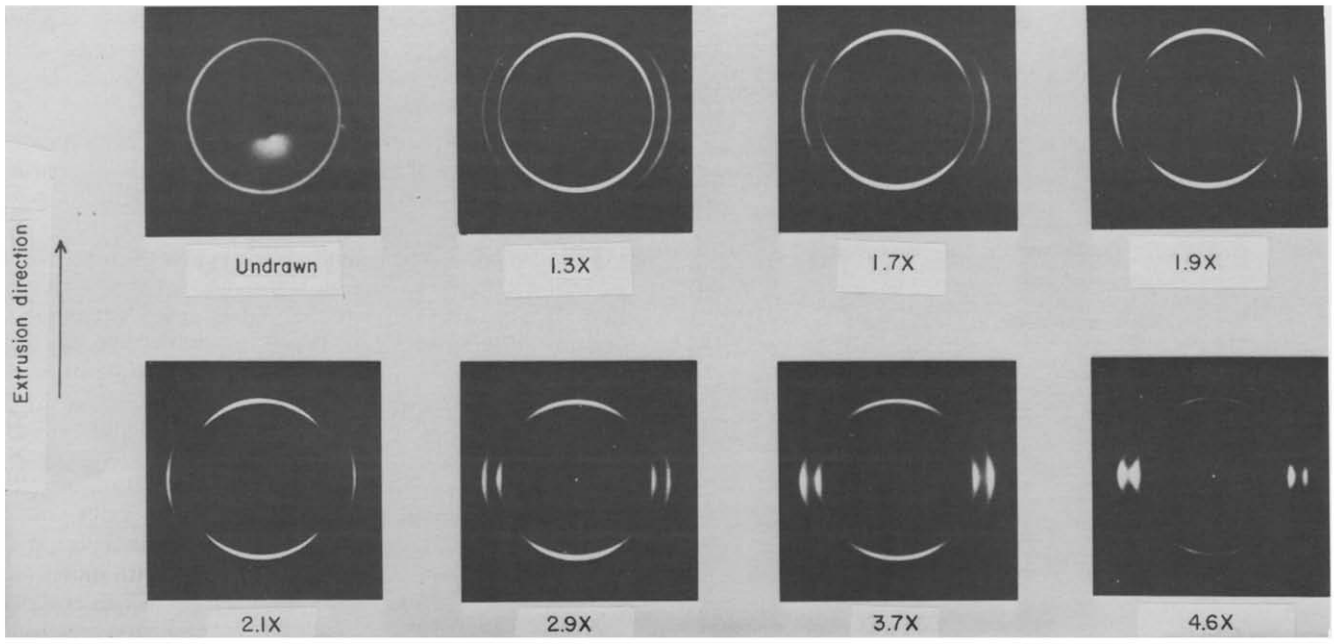

Figure 5 WAXD photographs of gel film with increasing draw ratio. X-ray beam normal to film plane

Figure 5 shows a series of WAXD photographs of gel film with increasing draw ratio; the X-ray beam is normal to the film plane. The undrawn film shows isotropy with (200) and (002) Debye rings. The outer (002) reflection is mixed with (202); for convenience, we refer to this as (002) only. At low draw ratio, up to 1.7×, the inner (200) reflection forms meridional arcs with broad azimuthal spread, while the outer equatorial (002) arcs are also broad but less intense. At a draw ratio of 1.9× the spread of these two arcs becomes narrower with simultaneous development of a faint (200) reflection at the equator. These equatorial arcs become prominent at a draw of 2.9× while the meridional (200) arcs become narrower in spread and split with maximum intensity centred at ~22° angle to the extrusion direction. Correspondingly, the azimuthal spread of (002) also becomes narrower. There is a faint reflection located diagonally with spacing nearly the same as that of the outer (002) reflection, which we identify as a weak (202) reflection. At higher draw of 4.6× the intensity of meridional (200) arcs decreases sharply when compared with their equatorial reflection.

Because of the complex orientation, we also examined both WAXD and SAXS with the X-ray beam transverse and parallel to the draw direction. The transverse diffraction shows patterns similar to those of the normal beam. At low draw, the parallel direction diffraction shows a weak orientation introduced during squeezing in gel film preparation with broad equatorial (200) arcs. On further drawing to 3.7×, it develops into a ring of uneven intensity around the draw direction. The system can be described as having double orientation of the crystals and is nearly centrosymmetric around the draw direction at higher draw.

In *Figure 5*, the equatorial (200) and (002) reflections can be identified as from the normal fibrous morphology with chain axes parallel to the uniaxial draw direction. The meridional (200) reflections are, however, from crystals with chain axis oriented perpendicular to draw. Here, these reflections are suggested to be from the fibrillar crystals which have the chain axis perpendicular to their flat surfaces.

To show how these diffraction patterns are obtained for these crystals, a reciprocal a^*–c^* lattice for the fibrillar crystals with chain axis oriented perpendicular to the draw direction is constructed. Since WAXD patterns are taken with a flat film camera and with CuKα radiation of wavelength 1.54 Å, the surface of the Ewald sphere is curved. The flat film diffraction pattern is then a distortion of the reciprocal lattice representation. However, this is small at low 2θ angle and it is useful to show the relative location of the reflections arising from the orientation.

The reciprocal lattice is oriented such that the (002) reflection is at the equator, while the (200) reflection is at the meridian (*Figure 6a*). At low draw, the fibrillar crystals rotate when subject to torque. The a-axis orients towards the draw direction. Since c^*-axis is perpendicular to a-axis, the measurement of the angle Ψ of the (002) reflection from the equator indicates the angle at which the a-axis is tilted towards the draw direction. Because of wide angular spread of the a-axis, there is a spread of Ψ with (200) and (002) reflections smeared over the meridian and equator, respectively. This results in WAXD patterns for draw $< 1.7\times$ as shown in *Figure 5*.

At higher draw, when the a-axis of the fibrillar crystals is oriented in the draw direction, Ψ becomes 0°. The diffraction pattern is then represented by a reciprocal lattice as in *Figure 6(b)*. In this case the meridional (200) reflections show intensity maxima at an angle of 22.5° from the draw direction, which is indeed observed at draw ratio 3.7× and higher indicating a complete a-axis orientation of the fibrillar crystals in draw direction. A weak (202) reflection appears diagonally in the reciprocal lattice and is also observed in the diffraction pattern.

If one now superimposes on *Figure 6(b)* the equatorial (200) and (002) reflections from the normal fibrous morphology with chain axis in the draw direction, the composite pattern obtained is consistent with the WAXD observations for draw ratio $> 3.7\times$ of *Figure 5*. Only the (002) reflection appears from crystals with both orientations, and therefore its intensity is enhanced.

Crystallite sizes along a-axis for both types of crystal orientations are measured from WAXD (200) line

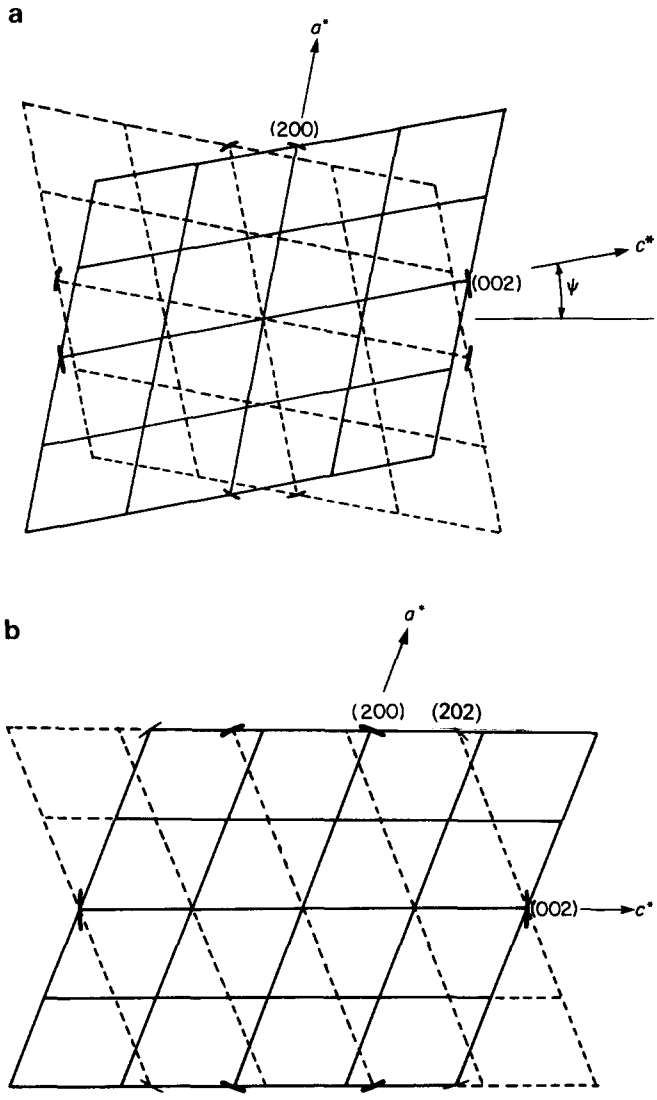

Figure 6 Reciprocal lattice representation of nylon-6 α-crystal showing relative position of (200), (002) and (202) reflections in WAXD. (a) Low draw, $<1.9\times$, (b) high draw, $>3.7\times$

broadening, and are shown in *Table 2*. Scherrer's equation was used after correction for instrumental broadening. It is assumed that broadening is due to crystallite size alone, neglecting lattice distortion. Therefore, the measured size is a lower bound. Measurement of (002) broadening is not suitable, as it is not a pure peak, but a mixture with (202) reflections. The crystallite sizes of fibrillar crystals along *a*-axis, as measured from broadening of meridional (200) reflection, showed a slight decrease on draw, from 101 Å at $1.9\times$ to $82\sim91$ Å at higher draw. For the equatorial (200) reflection, crystalline sizes remain fairly constant on draw, $62\sim69$ Å. This dimension may be interpreted as the lateral size of the drawn microfibril. Considering the interchain dimension of $4\sim5$ Å, this corresponds to about 15 nylon-6 chains in close lateral packing.

While the WAXD study gives us information on how chains are oriented at the level of unit cells, SAXS provides a view on orientation at the larger lamellar level. *Figure 7* shows SAXS patterns of gel film with increasing draw ratio. At a low draw of $1.3\times$, there is a marked change of the scattering pattern from nearly isotropic scattering for the undrawn state to a discrete four-point pattern along the equator. At higher draw, the four-point moves closer, while meridional scattering develops at $1.9\times$, thus giving a six-point scattering pattern. On further draw, the equatorial four-point merges into two-point at

Table 2 Crystallite sizes along *a*-axes for (200) equatorial and meridional reflections with increasing draw ratio

	Crystallite size $\bar{D}_{200}$ (Å)	
Draw ratio	Equatorial	Meridional
Undrawn	104	–
1.9	64	101
3.7	62	91
4.6	69	82
5.4	69	91

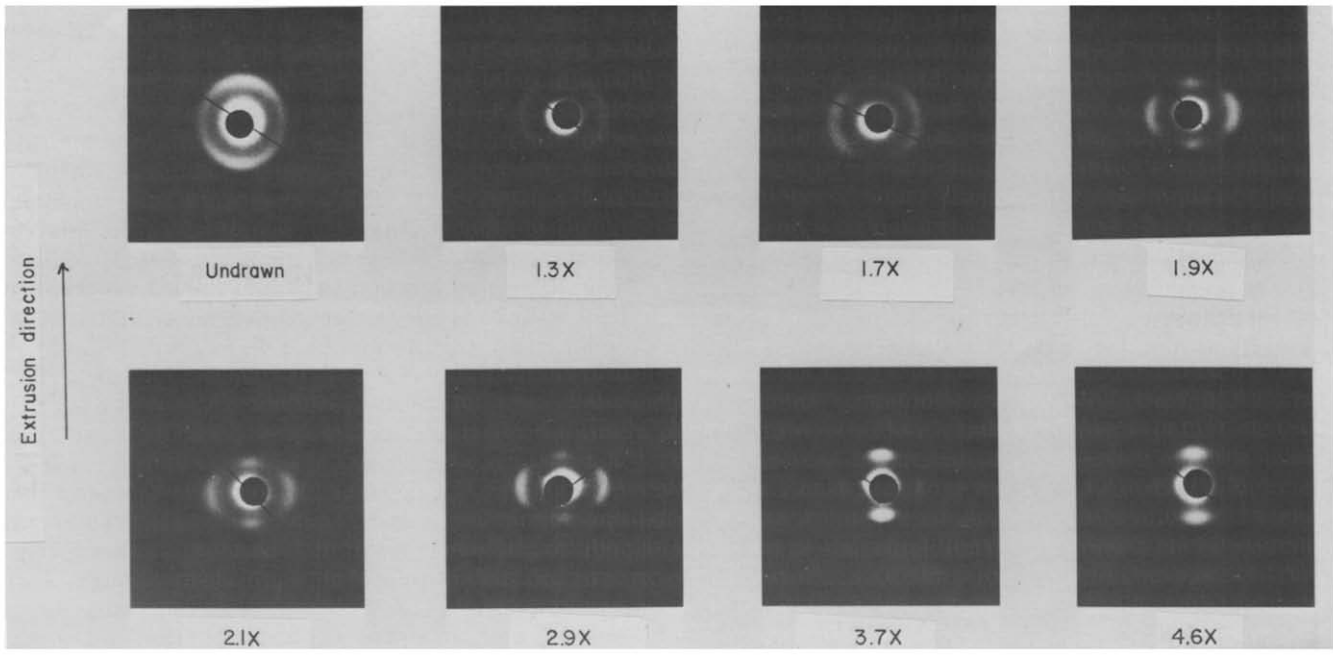

Figure 7 SAXS photographs of gel film with increasing draw ratio. X-ray beam normal to film plane

3.7×, giving a final four-point scattering along the meridian and equator.

To show that the equatorial scattering is not due to voids, the drawn film was immersed in benzyl alcohol (refractive index 1.54) for 14 days. It was then coated with paraffin oil to reduce solvent evaporation under vacuum while taking SAXS patterns. The patterns found are the same, indicating the equatorial scattering is not due to voids.

The measured lamellae long periods are tabulated in *Table 3*. The meridional long period of the drawn fibrous morphology is constant at ~85 Å. The equatorial periodicity of the fibrillar crystals is smaller but remains fairly constant at 65 Å on draw. Although Stamhuis and Pennings[14] reported the lateral dimension of such crystals to be 100~200 Å, thickness in the chain direction was not reported. The present periodicity is within the range for lamellar thickness reported for solution grown nylon-6 crystals[31].

The split angle, Ψ, of the equatorial scattering maxima gives the average angle of the long axis of fibrillar crystals to the draw direction. At a draw of 1.3×, the angle is 23.6° and decreases to 0° at 3.7× (*Table 4*). At 0° angle, the long axis (*a*-axis) of the fibrillar crystals is completely oriented in the draw direction. The SAXS results support the observation from WAXD.

From both WAXD and SAXS study, we showed double orientation in the drawn gel film. One population of the crystals has the chain axis parallel to the uniaxial draw direction. This type of crystal belongs to the fibrous morphology normally found in tensile drawing. The other crystal population has a chain axis perpendicular to draw, and they are identified as the fibrillar crystals associated with gelation. They rotate when subjected to torque during deformation, with the long axis orienting towards the draw direction. At low draw, <1.9×, they give rise to four-point SAXS pattern. On further drawing, when the long axis aligns in the draw direction, the four-point scattering merges into two equatorial maxima. Superimposed on this is the simultaneous development of the fibrous morphology with two-point meridional scattering. This explains the changes observed in the SAXS scatterings on drawing. Because hydrogen bonding

Table 3 Long period from SAXS of gel film with increasing draw ratio

	Long period (Å)	
Draw ratio	Equatorial	Meridional
Undrawn	64	—
1.3	66 66	87
1.9	66 65	86
2.1	68 66	87
2.8	66 66	85
3.7	65	87
4.6	62	82
5.4	62	81

Table 4 Change of angle, Ψ, between long axis of fibrillar crystals and draw direction

Draw ratio	Ψ (deg)
1.3	23.6
1.9	12.0
2.1	10.1
2.8	9.2
3.7	0

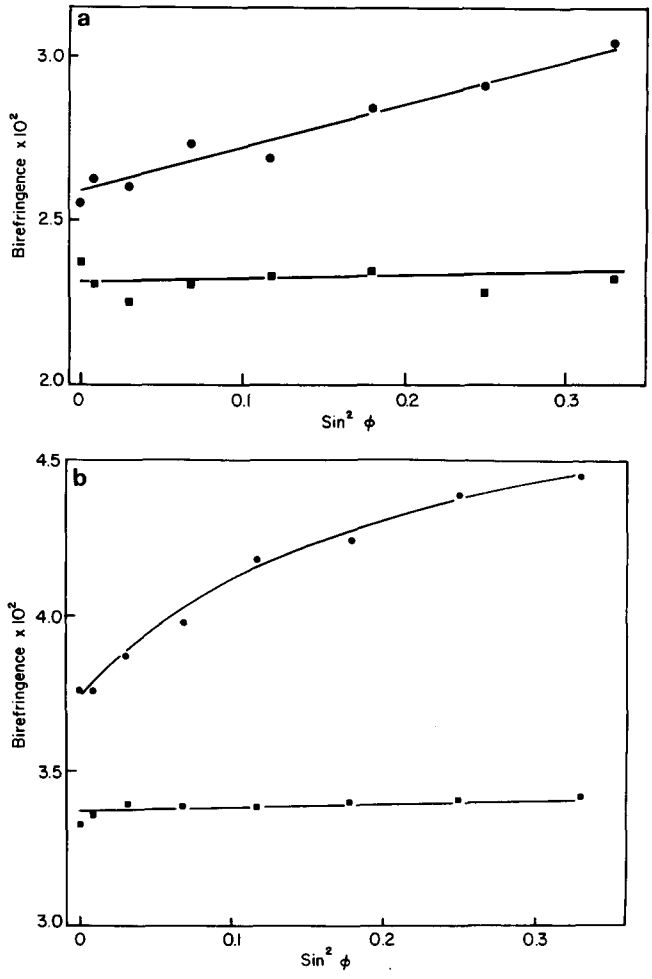

Figure 8 Birefringence as a function of tilt angle ϕ for unannealed (■), and annealed (●) gel: (a) draw ratio 2.9; (b) draw ratio 3.7

is also in the long axis of the fibrillar crystals, chains resist drawing until later stages, when 'fracture' possibly occurs, and transform part of the fibrillar crystals into fibrous morphology. This causes the depletion of the fibrillar crystals and therefore a decrease in their intensities in both WAXD and SAXS at high draw ratio.

Annealing behaviour

The drawn gel films were annealed with fixed ends at 190°C for 3 h. The modulus and birefringence increase slightly (*Figures 3* and *4*). WAXD and SAXS with the X-ray beam in normal and transverse directions are not significantly different from that of unannealed samples. However, when the beam is in the draw direction, superimposed on both (200) and (002) rings are intense arcs at the equator similar to those of the undrawn state of *Figure 2*. Reorientation of the fibrillar crystals occurs with chain axis partially reoriented normal to film plane, resulting in a more complicated orientation.

Birefringence of both unannealed and annealed gel film of draw 2.9× and 3.7× are shown in *Figures 8*(*a*) and (*b*) as a function of tilt angle, ϕ. For unannealed samples, there is only a slight increase in birefringence with ϕ, indicating a slight departure from isotropy around the uniaxial draw axis. On annealing, because of reorientation, the annealed samples not only show higher birefringence but this also increases with tilt angle. The increase is linear for draw 2.9× up to the angles measured but shows a tendency to reach plateau for draw 3.7×. For a biaxial orientation, birefringence at $\phi = 0°$ is different

from that at $\phi = 90°$. A plot of birefringence vs. $\sin^2\phi$ is linear and extrapolation to $\sin^2\phi = 1$ gives birefringence of the other axes pair[18]. Although the annealed 2.9 × film shows a linear increase, it is uncertain that this can be extrapolated to imply biaxial orientation, considering the annealed 3.7 × film, which shows a non-linear increase. Therefore, reorientation on annealing produce a much more complicated overall orientation.

CONCLUSIONS

A partially dried nylon-6 gel film was drawn by co-extrusion with poly(oxymethylene) as the outer billet at 150°C in an Instron rheometer up to a maximum draw ratio of 5.7 ×. Tensile moduli developed are comparable with those obtained in a similarly drawn solvent-cast nylon-6 film. The drawn gel film showed double orientation with one population of the crystals oriented with the chain axis in the draw direction. These crystals originated from the drawn fibrous morphology. The other crystal population had chain axis perpendicular to the draw direction and is identified as the initial fibrillar crystals. A deformation mechanism leading to this double orientation is proposed from the study of birefringence, WAXD and SAXS. Annealing at 190°C causes reorientation of the fibrillar crystals, resulting in a more complex orientation.

ACKNOWLEDGEMENT

We wish to express appreciation to the Office of Naval Research for the support of this research.

REFERENCES

1 Pennings, A. J. and Meihuizen, K. E. in 'Ultra-High Modulus Polymers', (Ed. A. Ciferri and I. M. Ward), Applied Science, 1979
2 Barham, P. J. *Polymer* 1982, **23**, 1112
3 Mackley, M. R. and Sapsford, G. S. in 'Developments in Oriented Polymers—I', (Ed. I. M. Ward), Applied Science, 1982
4 Smith, P. and Lemstra, P. J. *J. Polym. Sci., Polym. Phys. Edn.* 1981, **19**, 1007
5 Matsuo, M. and St. John Manley, R. *Macromolecules* 1982, **15**, 985
6 Cannon, C. G. *Polymer* 1982, **23**, 1123
7 Peguy, A. and St. John Manley, R. *Polymer* 1984, **25** (*Commun.*), 39
8 Grubb, D. T. 4th Cleveland Macromolecule Symposium, June 1983
9 Lloyd, D. J. in 'Colloid Chemistry, Vol. I', (Ed. J. Alexander), New York, 1926 (quoted in ref. 11)
10 Tager, A. 'Physical Chemistry of Polymers', MIR Publications, 1978
11 Hermans, P. H. in 'Colloid Science, Vol. II', (Ed. H. R. Kruyt), Elsevier, 1949
12 Keller, A. in 'Structure–Property Relationships of Polymeric Solids', (Ed. A. Hiltner), Plenum Press, 1983
13 Lemstra, P. J. and Smith, P. *Br. Polym. J.* 1980, **12**, 212
14 Stamhuis, J. E. and Pennings, A. J. *Br. Polym. J.* 1978, **10**, 221
15 Chuah, H. H. and Porter, R. S. *J. Polym. Sci., Polym. Phys. Edn.* 1984, **22**, 1353; Zachariades, A. E., Watts, M. P. C., Kanamoto, T. and Porter, R. S. *J. Polym. Sci., Polym. Lett. Edn.* 1979, **17**, 485
16 Zachariades, A. E., Griswold, P. D. and Porter, R. S. *Polym. Eng. Sci.* 1979, **19**, 441
17 Stein, R. S. *J. Polym. Sci.* 1957, **24**, 383
18 Desper, C. R. *Ph.D. Thesis*, University of Massachusetts, 1966
19 Shimada, T. and Porter, R. S. *Polymer* 1981, **22**, 1124
20 Kyotani, M. *J. Macromol. Sci., Phys.* 1982, **B21**, 275
21 Todoki, M. and T. Kawaguchi, T. *J. Polym. Sci., Polym. Phys. Edn.* 1977, **15**, 1507
22 Urbanczyk, G. W. *J. Polym. Sci.* 1962, **59**, 215
23 Pereira, J. R. C. and Porter, R. S. *J. Polym. Sci., Polym. Phys. Edn.* 1983, **21**, 1147
24 Chuah, H. H., DeMicheli, R. E. and Porter, R. S. *J. Polym. Sci., Polym. Lett. Edn.* 1983, **21**, 791
25 Glenz, W., Morosoff, N. and Peterlin, A. *J. Polym. Sci., Polym. Lett. Edn.* 1971, **9**, 211
26 Fujimoto, F. *et al. Nippon Sen'i Kikai Gakkai* 1973, **19**, 1
27 Berghman, H., Govaerts, F. and Overbergh, N. *J. Polym. Sci., Polym. Phys. Edn.* 1979, **17**, 1251
28 Guerrero, S. J., Keller, A., Soni, P. L. and Geil, P. H. *J. Polym. Sci., Polym. Phys. Edn.* 1980, **18**, 1533
29 Atkins, E. D. T. *et al. Colloid Polym. Sci.* 1984, **262**, 22
30 Bonart, R. and Hoffman, K. *Colloid Polym. Sci.* 1982, **260**, 268
31 Wunderlich, B. 'Macromolecular Physics, Vol. I', Academic Press, 1973